Progress In Electromagnetics Research C, Vol. 53, 135–144, 2014

A New Type of High-Power Microwave Impedance Tuner Based on Load-Pull with a Rapid Calibration Method

Peng Cheng*, Lu Sun, Jia-Li Wang, Long-Long Xue, Chun-Yang Zhou, and Xiao-Long Wang

Abstract—For the measurement of microwave device in high-power, traditional methods are inefficient, inaccurate and not on-line real-time measurement. A new type of high-power microwave impedance tuner (26.5 GHz $\sim$ 40 GHz) based on load-pull technique and a corresponding rapid calibration method based on curve fitting are proposed. A new structure using increased width rectangular waveguide slotted in the center is adopted as the main transmission line. In order to prevent the leak of electromagnetic waves transferring in rectangular waveguide, two choke grooves are added in upper cover plate of the waveguide cavity. The results (standing wave ratio range of 1.02 $\sim$ 10.98, insertion loss of 0.063 dB at minimum standing wave ratio) show by practical measurement that this structure and method are feasible. The device can meet the requirement of design, and the new method has less time for calibration.

1. INTRODUCTION

With the progress of science and technology, information industry is developing rapidly. The RF/MW (Radio Frequency/Microwave) semiconductor device has more and more extensive application. High-power microwave device is indispensable in microwave communication, electronic countermeasures, satellite radar system, etc. Therefore, it is more and more important for accurate measurements of the parameters, especially, in high-power state. The traditional test method is to measure the scattering parameters of high-power devices in small signal with the vector network analyzer (VNA) and to calculate the scattering parameters in large signal [1–4]. And it has low precision and efficiency. Power amplifier test system (PATS) which is manufactured by Maury and Focus holds a leading position in the industry in the world today. This paper introduces the structure and principle of a new type of high-power microwave impedance tuner based on load-pull technique, and the feasibility of a rapid calibration method based on the actual measurement data.

2. PRINCIPLE

In linear system, in order to get maximum gain or transmission power, conjugate match is adopted in the input/output [5–7]. The tuner proposed in this paper is placed at both ends of the device under test (DUT). Under the condition of given frequency, source/load impedance is tuned by tuner, at the same time input/output power is measured by power meter. Maximum transmission power is obtained after data processing [8–10]. Based on the calibration data before measurement, we can get scattering parameters of the DUT at this frequency. The principle block diagram of load-pull is shown in Figure 1.

The principle of the tuner proposed in this paper is the same as that of single-stub tuner. Single-stub tuner consists of short or open circuit terminal line (length of m) in parallel or series, n from the

Received 31 March 2014, Accepted 1 September 2014, Scheduled 12 September 2014
* Corresponding author: Peng Cheng (chengpeng353@qq.com).
The authors are with Institute of Electro-Mechanical Engineering, Xidian University, 2 South Taibai Road, Xi'an, Shaanxi 710071, P. R. China.

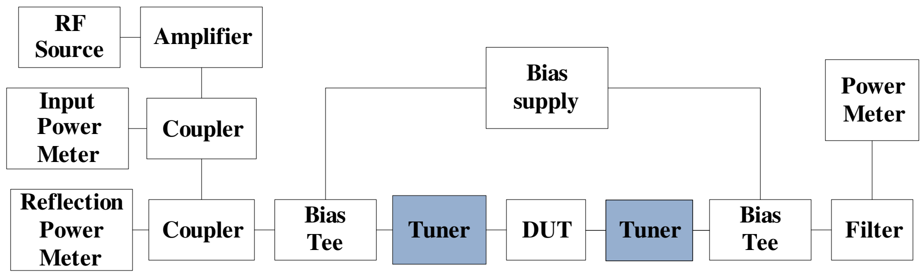

Figure 1. The principle block diagram of load-pull.

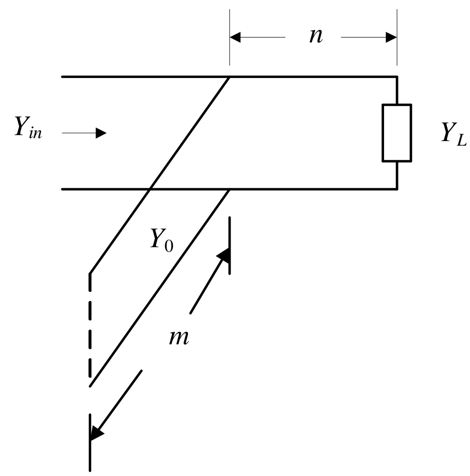

Figure 2. Structure of single-stub tuner.

load, as shown in Figure 2. In a single-stub tuner, its susceptance can be adjusted by two adjustable parameters, which are m and n. Appropriate distance (n) is selected so that admittance, from the stub to the load, is $Y_{in} = Y_0 + jB$, then appropriate length (m) of stub is selected so that susceptance is $Y_0 = -jB$, so as to achieve matching [11–14].

3. STRUCTURE AND PARAMETERS

The new type of high-power microwave impedance tuner proposed in this paper consists of BJ-320 rectangular waveguides (size of 7.112 mm × 3.556 mm, cut-off frequency of 21.053 GHz, the dominant mode frequency range of 26.3 GHz ∼ 40 GHz), high precision stepping motor, metal probe (13 mm × 2 mm × 0.5 mm), computer interface, etc., as shown in Figure 3. The positioning accuracy can reach the precision of micrometer level by high precision step motor, thus ensuring good repeatability. The physical map of the tuner is shown in Figure 4. The design index in detail is as follows:

Frequency range: 26.5 GHz ∼ 40 GHz.

Minimum standing wave ratio (SWR) in port: 1.2 : 1.

Maximum SWR in port: 10 : 1.

Insertion loss: $\leq$ 1.0 dB (minimum standing wave ratio).

In order to ensure the stub line connecting the load can be moved in main transmission line. We select increased width rectangular waveguide slotted in the center as the main transmission line, and insert a longitudinal probe as the parallel stub line. Susceptance changes with probe insertion depth. As shown in Figure 3. Distance n changes with probe horizontal location. Length m changes with probe insertion depth.

In order to prevent the leak of electromagnetic waves transferring in rectangular waveguide, two choke grooves are added in upper cover plate of the waveguide cavity [15–19]. Its structure is shown in Figure 5.

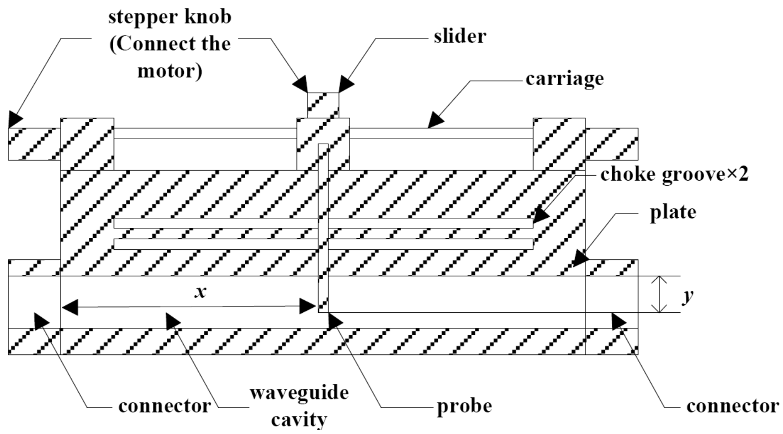

Figure 3. Structure of the tuner.

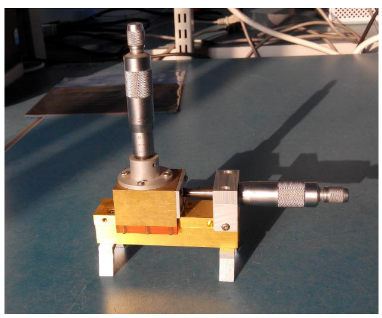

Figure 4. Physical map of the tuner.

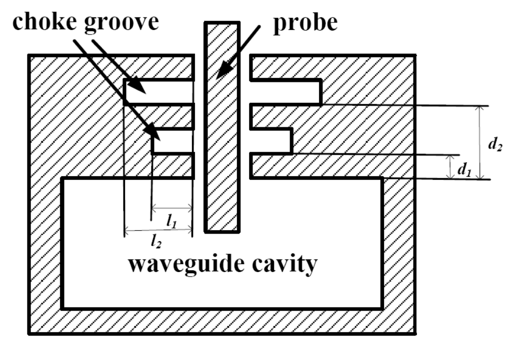

Figure 5. Structure of choke groove.

The design of choke groove is mainly based on the theory of half-wavelength short-circuited line. There are two rectangular grooves on both sides of the probe slot with length of $\lambda/4$. The distance between the lower choke groove and the surface of the waveguide cavity is also $\lambda/4$. In this way, the choke groove can be considered as transmission line with low impedance whose end is short-circuited [20]. The schematic diagram and equivalent circuit of the choke groove are shown in Figure 6.

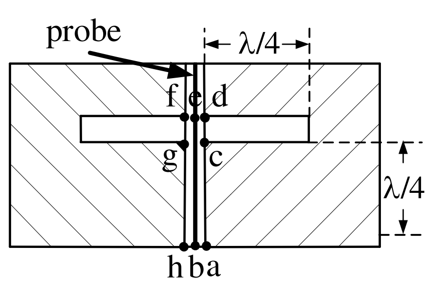

Figure 6. Schematic diagram of proposed choke groove configuration.

Boundary conditions of the waveguide wall are changed by the slit in the center of the waveguide surface, which is equivalent to the introduction of a resistive component (R_k) in the wave impedance (Z_{TE}) of rectangular waveguide in mode TE_{mn}. What we wanted is the resistive component between both ends of slit $(a, h)Z_{ah} = 0$, no matter what the value of the component R_k is. As shown in Figure 6, the line of b-e represents the probe inserted into the slit, and a, c, d and f, g, h are the endpoints on choke groove wall. From Figure 6, viewing from c-d, the choke groove is $\lambda/4$ short-circuited line, so

$Z_{cd} = \infty$, i.e., $Z_{ce} = Z_{cd} + R_k = \infty$. So from c-e, the circuit is equal to open. It is the same case with Z_{cg} (so $Z_{cg} = \infty$) because of symmetry. Similarly, it is a $\lambda/4$ short circuit viewing from the c-g, so $Z_{ah} = 0$, and it doesn't change with R_k. This ensures the effective electrical connection of slit in the waveguide, and prevents the leak of electromagnetic waves transferring in rectangular waveguide.

The choke groove based on $\lambda/4$ transmission line has the properties of not only no radiation, no power loss, no reflection, but also frequency selective which means narrow bandwidth. In order to meet the requirement of bandwidth, the impedance of the first $\lambda/4$ transmission line is designed higher than the second $\lambda/4$ one, the width of the probe slot is 0.7 mm and the height of rectangle groove is 0.5 mm. Two choke grooves are designed to match the high and low frequency bands respectively. The initial size of two choke grooves is given by (1).

$$\begin{cases} l_1 + d_1 = \lambda_1/2 \\ l_2 + d_2 = \lambda_2/2 \end{cases} \tag{1}$$

where l_1, l_2 are depth of the two choke grooves; d_1, d_2 are the height of the surface of two choke grooves from the upper surface of the waveguide cavity, as shown in Figure 5; λ_1, λ_2 are the wavelengths that correspond to the high and low operating frequency band, respectively. According to the indexes of this paper, the initial value of two choke grooves is given by (2).

$$\begin{cases} l_1 = 1.9\,\text{mm} \\ l_2 = 3\,\text{mm} \\ d_1 = 1.278\,\text{mm} \\ d_2 = 3.056\,\text{mm} \end{cases} \tag{2}$$

The simulation in HFSS (High Frequency Structure Simulator) shows that the properties of waveguide with choke groove are the same as that of BJ-320 waveguide, when probe is completely detached from waveguide. And it can meet the minimum SWR 1.2 : 1 and insertion loss ≤ 1.0 dB (in minimum SWR).

4. MEASUREMENT AND CALIBRATION

Tuner should be calibrated by VNA before the actual measurement for DUT. The location and the scattering parameters of tuner are recorded when the probe is in one position, and this process is repeated as many times as possible. Then we can create a database of the relationship between the probe location and the scattering parameters. In actual measurement, the scattering parameters corresponding to the probe location can be obtained by querying the database, thus obtaining the parameter of DUT. This calibration method has shortcoming of huge amount of data and time-consuming. Therefore, a rapid calibration method is proposed.

Theoretically, modulus value of the scattering parameter is unchanged with the horizontal movement (x_0) of the probe in x direction; its phase variation is as follows:

$$\begin{cases} \varphi_{11}(x) = \varphi_{11}(x_0) + \dfrac{2\pi(x - x_0)}{\lambda_g/2} \\ \varphi_{12}(x) = \varphi_{12}(x_0) \\ \varphi_{21}(x) = \varphi_{21}(x_0) \\ \varphi_{22}(x) = \varphi_{22}(x_0) + \dfrac{2\pi(x - x_0)}{\lambda_g/2} \end{cases} \tag{3}$$

where λ_g is waveguide wavelength. So only measuring a horizontal position and a group of vertical positions for the probe of tuner, tuner's scattering parameter variation with insertion depth can be obtained. Then the scattering parameters of tuner at any position can be calculated by (3). The connection of rapid calibration is shown in Figure 7. First, calibration kit is connected (Figure 7(a)) for VNA's calibration. Then after connecting the tuner as shown in Figure 7(b), tuner can be calibrated by the above method.

We have measured the tuner with VNA and get the scattering data of tuner in 341 (11×31) different positions at 109 frequency points (26.5 GHz $\sim$ 40 GHz, stepper 0.125 GHz) for verifying the

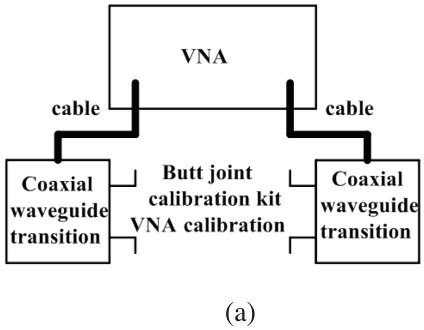

Figure 7. Connection of rapid calibration. (a) Connection of calibration kit. (b) Connection of tuner.

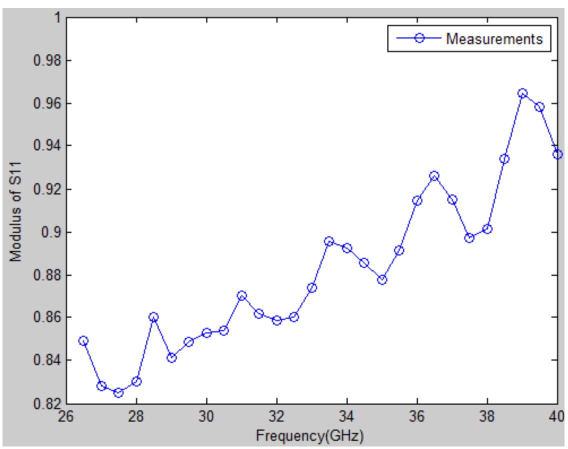

Figure 8. Relationship between frequency and modulus of S_{11} ($x = 6\,\text{mm}$, $y = 2.4\,\text{mm}$).

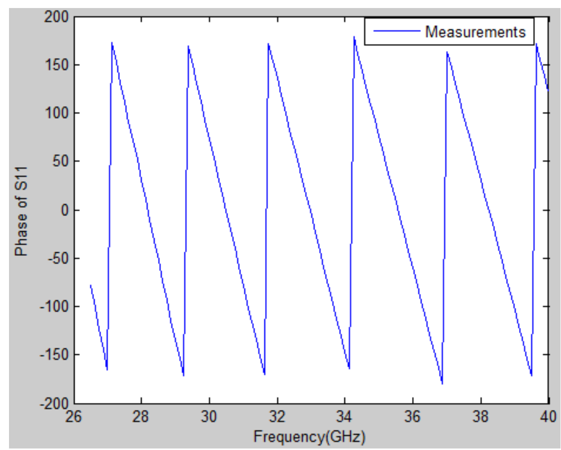

Figure 9. Relationship between frequency and phase of S_{11} ($x = 6\,\text{mm}$, $y = 2.4\,\text{mm}$).

feasibility of this rapid calibration method. The probe's vertical positions are from 0 mm to 3 mm with a step of 0.3 mm, and its horizontal positions are from 0 mm to 15 mm with a step of 0.5 mm. The tuner manufactured this time is just to verify whether the structure of this new type of tuner is feasible, so there is no specialized device for positioning the probe on the tuner. Only two micrometers are used to determine the horizontal and vertical positions of the probe. Therefore, there is an error in determining the actual positions of the probe.

With $x = 6\,\text{mm}$, $y = 2.4\,\text{mm}$, the relationship between frequency and S_{11}, S_{21} is shown in Figures 8, 9, 10 and 11.

Tables 1 and 2 show the scattering parameter S_{11}'s modulus and phase measured of the tuner at the frequency f_0 of 33 GHz and the horizontal position x of 6 mm, 7 mm, 8 mm, 9 mm respectively. They are processed in Matlab.

The data ($f_0 = 33\,\text{GHz}$, $x = 6\,\text{mm}$) are fitted by the least squares method. Fitting results are shown in Figures 12 and 13.

The fifth order polynomial function of S_{11}'s modulus with vertical depth (y) as independent variable is given by (4).

$$\begin{cases} f\left(y\right) = p_1 y^5 + p_2 y^4 + p_3 y^3 + p_4 y^2 + p_5 y + p_6 \\ p_1 = 0.01878, \quad p_2 = -0.1514 \\ p_3 = 0.3368, \quad p_4 = -0.0588 \\ p_5 = 0.03188, \quad p_6 = 0.01089 \end{cases} \tag{4}$$

The sixth order polynomial piecewise function of S_{11}'s phase with vertical depth (y) as independent

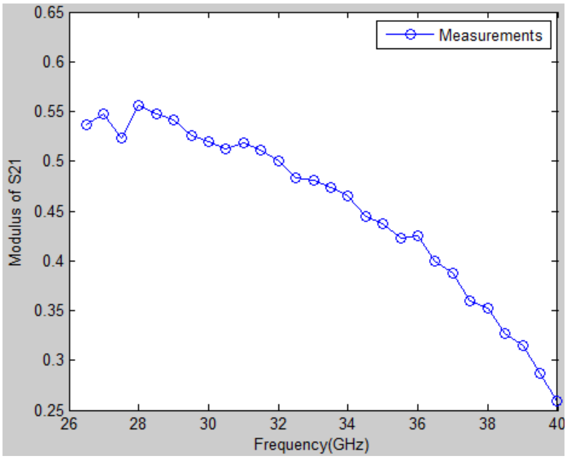

Figure 10. Relationship between frequency and modulus of S_{21} ($x = 6$ mm, $y = 2.4$ mm).

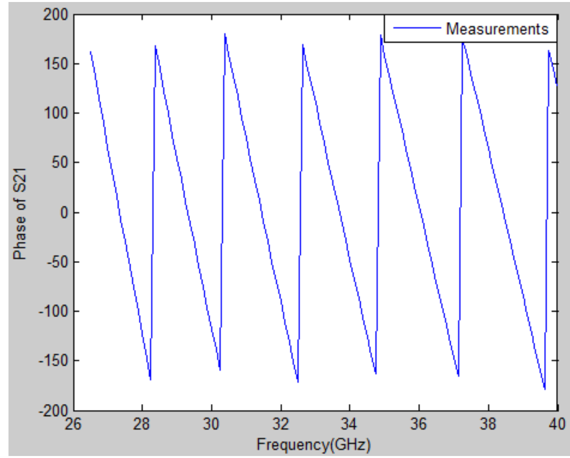

Figure 11. Relationship between frequency and phase of S_{21} ($x = 6$ mm, $y = 2.4$ mm).

Table 1. Scattering parameter S_{11}'s modulus measured of the tuner ($f_0 = 33$ GHz, $x = 6$ mm, 7 mm, 8 mm, 9 mm).

insertion depth y (mm)	$x = 6$ mm	$x = 7$ mm	$x = 8$ mm	$x = 9$ mm
0.0	0.011 762	0.011 829	0.011 437	0.010 470
0.3	0.019 714	0.022 558	0.019 489	0.010 660
0.6	0.067 776	0.069 992	0.066 134	0.053 415
0.9	0.145 878	0.150 558	0.144 096	0.130 102
1.2	0.287 074	0.295 364	0.292 482	0.277 736
1.5	0.424 457	0.441 746	0.438 697	0.418 030
1.8	0.618 432	0.642 596	0.641 388	0.618 866
2.1	0.758 307	0.729 189	0.791 656	0.770 475
2.4	0.873 942	0.899 805	0.894 224	0.863 295
2.7	0.945 611	0.962 078	0.961 908	0.933 814
3.0	0.968 825	0.972 307	0.978 964	0.936 789

Table 2. Scattering parameter S_{11}'s phase measured of the tuner ($f_0 = 33$ GHz, $x = 6$ mm, 7 mm, 8 mm, 9 mm).

insertion depth y (mm)	$x = 6$ mm	$x = 7$ mm	$x = 8$ mm	$x = 9$ mm
0.0	−1.815 99	−6.344 640	−9.234 55	−8.228 78
0.3	22.651 94	−6.511 057	−38.042 5	−69.410 2
0.6	40.498 94	−13.778 46	−66.028 2	54.275 71
0.9	33.328 62	−22.389 33	−79.706 0	38.061 72
1.2	40.109 45	−16.173 39	−75.068 1	43.993 62
1.5	17.281 45	−41.446 48	78.966 55	19.050 16
1.8	22.218 84	−37.551 37	83.084 45	21.597 37
2.1	10.132 56	−53.200 91	69.091 05	6.613 94
2.4	−5.739 44	−66.195 80	52.352 68	−9.290 10
2.7	2.355 314	−57.919 31	60.360 73	−1.388 05
3.0	−15.089 9	−74.86924	43.875 61	−17.066 7

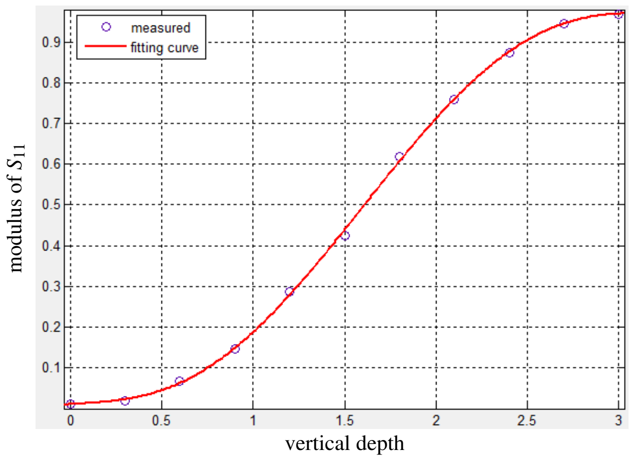

Figure 12. Fitting curve of S_{11}'s modulus ($f_0 =$ 33 GHz, $x = 6$ mm).

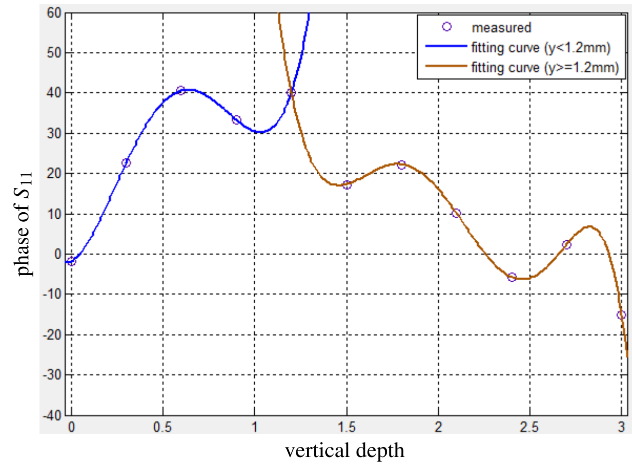

Figure 13. Fitting curve of S_{11}'s phase ($f_0 =$ 33 GHz, $x = 6$ mm).

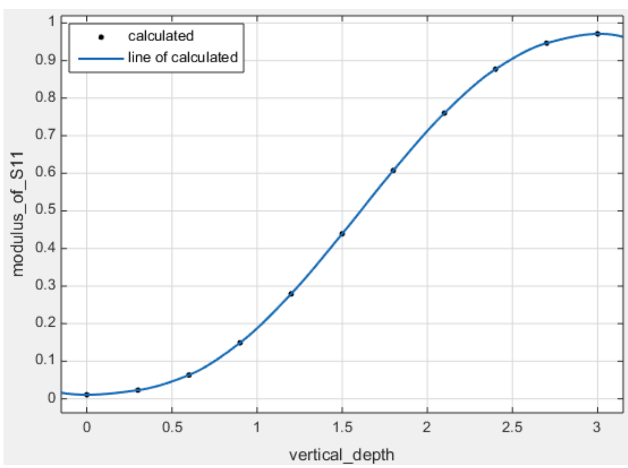

Figure 14. Calculated modulus of S_{11} ($f_0 =$ 33 GHz, $x = 6$ mm).

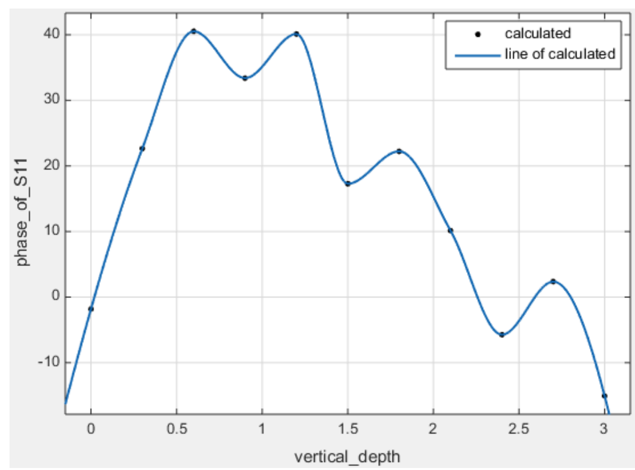

Figure 15. Calculated phase of S_{11} ($f_0 =$ 33 GHz, $x = 6$ mm).

variable is given by (5).

$$\begin{cases} f(y) = p_1 y^6 + p_2 y^5 + p_3 y^4 + p_4 y^3 + p_5 y^2 + p_6 y + p_7 \\ y \leq 12 \begin{cases} p_1 = 0, \quad p_2 = 0, \quad p_3 = 295.1 \\ p_4 = -644.7, \quad p_5 = 357.6 \\ p_6 = 24.35, \quad p_7 = -1.816 \end{cases} \\ y > 12 \begin{cases} p_1 = -91.95, \quad p_2 = 926.6 \\ p_3 = -3531, \quad p_4 = 6057, \quad p_5 = -3755 \\ p_6 = -1206, \quad p_7 = 1719 \end{cases} \end{cases} \tag{5}$$

At 33 GHz, with vertical depth unchanged and horizontal displacement changed, the variation of modulus and phase of S_{11} is given by (6).

$$\begin{cases} |S_{11}(x, y)| = |S_{11}(x_0, y)| \\ \phi_{11}(x, y) = \phi_{11}(x_0, y) - \frac{4\pi}{\lambda_g}(x - x_0) \end{cases} \tag{6}$$

where x_0 is initial horizontal, i.e., x_0= 6mm, and λ_g is waveguide wavelength, i.e.,

$$\lambda_g = \frac{\lambda_0}{\sqrt{1 - (\lambda_0/2a)^2}} \tag{7}$$

where λ_0 is wavelength of electromagnetic waves at 33 GHz, and a is waveguide width, i.e., $\lambda_0 = 9.085\,\text{mm}$, $a = 7.112\,\text{mm}$. Substituting them into (7), we can get $\lambda_g = 11.806\,\text{mm}$. Then according to (4), (5) and (6), the scattering parameter S_{11} at 33 GHz with probe at any position can be obtained. Modulus and phase of S_{11} ($x = 6\,\text{mm}$) are shown in Figures 14 and 15 respectively.

The absolute error is obtained by the subtraction of the measurement in Tables 1, 2 from the calculated value. The absolute error and mean square error (MSE) are shown in Tables 3 and 4.

According to Tables 3 and 4, we find that scattering parameter S_{11} has small errors. The first three groups of data ($y = 0\,\text{mm}$, 0.3 mm, 0.6 mm) are abnormal. According to the analysis, the positioning device of tuner is manual, not precise enough, and probe may not be inserted in waveguide cavity with

Table 3. Error of scattering parameter S_{11}'s modulus of the tuner ($f_0 = 33\,\text{GHz}$, $x = 6\,\text{mm}$, 7 mm, 8 mm, 9 mm).

insertion depth y (mm)	$x = 6\,\text{mm}$	$x = 7\,\text{mm}$	$x = 8\,\text{mm}$	$x = 9\,\text{mm}$
0.0	0.000 872	0.000 939	0.000 547	0.000 419
0.3	0.003 360	0.000 516	0.003 585	0.012 414
0.6	0.004 338	0.006 554	0.002 696	0.010 022
0.9	0.003 358	0.001 321	0.005 140	0.019 134
1.2	0.007 822	0.016 112	0.013 230	0.001 515
1.5	0.014 800	0.002 488	0.000 560	0.021 227
1.8	0.010 928	0.035 092	0.033 884	0.011 362
2.1	0.001 879	0.030 997	0.031 469	0.010 289
2.4	0.002 986	0.022 876	0.017 294	0.013 634
2.7	0.000 644	0.015 822	0.015 652	0.012 442
3.0	0.002 244	0.001 237	0.007 894	0.034 280
MSE	0.006 465	0.017 266	0.016 424	0.016 024

Table 4. Error of scattering parameter S_{11}'s phase of the tuner ($f_0 = 33\,\text{GHz}$, $x = 6\,\text{mm}$, 7 mm, 8 mm, 9 mm).

insertion depth y (mm)	$x = 6\,\text{mm}$	$x = 7\,\text{mm}$	$x = 8\,\text{mm}$	$x = 9\,\text{mm}$
0.0 (abandon)	0.000 001	56.455 829	65.449 613	3.459 382
0.3 (abandon)	0.004 465	31.817 001	61.269 964	89.113 274
0.6 (abandon)	0.020 817	6.686 247	15.420942	16.709 357
0.9	0.055 180	5.211 325	8.879 104	7.631 317
1.2	0.000 000	4.701 621	6.791 303	6.837 576
1.5	0.000 000	2.256 531	3.654 034	4.722 113
1.8	0.000 000	1.214 248	2.834 550	2.331 932
2.1	0.000 000	2.349 007	0.927 427	0.565 213
2.4	0.000 000	0.528 109	0.061 066	0.597 244
2.7	0.000 000	0.709 839	0.025 646	0.789 956
3.0	0.000 000	1.205 174	0.934 500	0.976 649
MSE	0.019 509	2.819 187	4.302 394	4.107 611

micrometer readings of 0.6 mm, so that these measurements are not accurate. However, it can be seen from the other data that this rapid calibration method is feasible. And motor stepper and computer, which will be used in future, can make calibration more accurate. It will take 31 times longer to get these data (109 frequencies, 31×11 positions) by Maury's instrument, so this rapid calibration method is time-saving.

5. CONCLUSIONS

This paper presents a new type of high-power microwave impedance tuner based on load-pull technique and its corresponding rapid calibration method. By testing, this new structure of increased width rectangular waveguide slotted in the center and the rapid calibration method based on curve fitting are proved to be feasible and effective. The choke groove also effectively inhibits leakage of electromagnetic. Grating-ruler, stepper motor and computer will be used in the future work for precise positioning as soon as possible, so that the calibration formula can be optimized, and calibration becomes more accurate.

ACKNOWLEDGMENT

The authors would like to thank the 41st Institute of China Electronics Technology Group Corporation for manufacture and measurement. Their assistances are gratefully acknowledged.

REFERENCES

1. Hashmi, M. S. and F. M. Ghannouchi, "Introduction to load-pull systems and their applications," *IEEE Instrumentation & Measurement Magazine*, Vol. 16, No. 1, 30–36, 2013.
2. Ferrero, A. and M. Pirola, "Harmonic load-pull techniques: An overview of modern systems," *IEEE Microwave Magazine*, Vol. 14, No. 4, 116–123, Jun. 2013.
3. Teppati, V., A. Ferrero, and U. Pisani, "Recent advances in real-time load-pull systems," *IEEE Transactions on Instrumentation and Measurement*, Vol. 57, No. 11, 2640–2646, Jun. 2008.
4. Hone, T. M., S. Bensmida, and K. A. Morris, "Controlling active load-pull in a dual-input inverse load modulated doherty architecture," *IEEE Transactions on Microwave Theory and Techniques*, Vol. 60, No. 6, 1797–1804, 2012.
5. Bengtsson, O., L. Vestling, and J. Olsson, "A computational load-pull method with harmonic loading for high-efficiency investigations," *Solid-State Electronics*, Vol. 53, No. 1, 86–94, 2009.
6. Hoefer, W. J. R. and M. N. Burton, "Closed-form expressions for the parameters of finned and ridged waveguides," *IEEE Transactions on Microwave Theory and Techniques*, Vol. 30, No. 12, 2190–2194, 1982.
7. Teppati, V. and C. R. Bolognesi, "Evaluation and reduction of calibration residual uncertainty in load-pull measurements at millimeter-wave frequencies," *IEEE Transactions on Instrumentation and Measurement*, Vol. 61, No. 3, 817–822, Mar. 2012.
8. Albasha, L., "Technique for harmonic minimisation in high-power MMIC antenna switches using load-pull tuners," *IET Microw. Antennas Propag.*, Vol. 5, No. 10, 1131–1135, 2011.
9. Moravek , O. and K. Hoffmann, "Improvement to load-pull technique for design of large-signal amplifier in K band," *Radioengineering*, Vol. 20, No. 4, 828–831, 2011.
10. Vadala, V., A. Raffo, S. Di Falco, and G. Bosi, "A load-pull characterization technique accounting for harmonic tuning," *IEEE Transactions on Microwave Theory and Techniques*, Vol. 61, No. 7, 2695–2704, 2013.
11. Hoarau, C., P.-E. Bailly, J.-D. Arnould, P. Ferrari, and P. Xavier, "Accurate measurement method for characterisation of RF impedance tuners," *Electronics Letters*, Vol. 43, No. 25, 1434–1436, 2007.
12. Andersson, C. M., M. Thorsell, and N. Rorsman, "Nonlinear characterization of varactors for tunable networks by active source-pull and load-pull," *IEEE Transactions on Microwave Theory and Techniques*, Vol. 59, No. 7, 1753–1760, 2011.

13. Roff, C., J. Graham, J. Sirois, and B. Noori, "A new technique for decreasing the characterization time of passive load-pull tuners to maximize measurement throughput," *2008 72nd ARFTG Microwave Measurement Symposium*, 92–96, Dec. 9–12, 2008.
14. Bonino, S., V. Teppati, and A. Ferrero, "Further improvements in real-time load-pull measurement accuracy," *IEEE Microwave and Wireless Components Letters*, Vol. 20, No. 2, 121–123, 2010.
15. Ghannouchi, F. M., M. S. Hashmi, S. Bensmida, and M. Helaoui, "Loop enhanced passive source- and load-pull technique for high reflection factor synthesis," *IEEE Transactions on Microwave Theory and Techniques*, Vol. 58, No. 11, 2952–2959, 2010.
16. Hashmi, M. S., A. L. Clarke, S. P. Woodington, J. Lees, J. Benedikt, and P. J. Tasker, "An accurate calibrate-able multiharmonic active load-pull system based on the envelope load-pull concept," *IEEE Transactions on Microwave Theory and Techniques*, Vol. 58, No. 3, 656–664, 2010.
17. Browne, J., "Load-pull system aids nonlinear device modeling," *Microwaves and RF*, Vol. 48, No. 8, 90–92, 2009.
18. Vaha-Heikkila, T., J. Varis, J. Tuovinen, and G. M. Rebeiz, "A 20–50 GHz RF MEMS single-stub impedance tuner," *IEEE Microwave and Wireless Components Letters*, Vol. 15, No. 4, 205–207, 2005.
19. Sun, L., J. S. Zhan, and J. L. Wang, "A waveguide design of microwave high power passive tuner," *Advanced Materials Research.*, Vols. 588–589, 856–859, 2012.
20. Albasha, L., "Technique for harmonic minimisation in high-power MMIC antenna switches using load-pull tuners," *IET Microw. Antennas Propag.*, Vol. 5, No. 10, 1131–1135, 2011.